Journal of Solid State Chemistry 181 (2008) 2178–2184

Contents lists available at ScienceDirect

Journal of Solid State Chemistry

journal homepage: www.elsevier.com/locate/jssc

Syntheses, crystal structures and properties of two 1-D cadmium(II) coordination polymers based on 1,1′-(1,3-propanediyl)bis-1H-benzimidazole

Huaixia Yang [a], Xiangru Meng [b], Yun Liu [b], Hongwei Hou [b,*], Yaoting Fan [b], Xiaoqing Shen [b]

[a] Pharmacy College, Henan University of Traditional Chinese Medicine, Zhengzhou, Henan 450008, PR China
[b] Department of Chemistry, Zhengzhou University, Zhengzhou, Henan 450052, PR China

ARTICLE INFO

Article history:
Received 23 February 2008
Received in revised form
26 April 2008
Accepted 29 April 2008
Available online 16 May 2008

Keywords:
Coordination polymer
Crystal structure
Antimicrobial activity
Non-isothermal kinetics

ABSTRACT

The combination of framework-builders 1,1′-(1,3-propanediyl)bis-1H-benzimidazole (pbbm), Cd(II) ion and framework-regulator ClO_4^- or SO_4^{2-} provides two new coordination polymers $[Cd(pbbm)_2(ClO_4)_2]_n$(**1**) and $\{[Cd(pbbm)SO_4(H_2O)_2]\cdot CH_3OH\}_n$(**2**). Both of them display 1-D chain framework, but their detailed structures are clearly different from each other. **1** displays a 1-D ribbon of rings framework, **2** features an interesting infinite 1-D looped chain structure composed of two kinds of rings, the smaller 8-membered ring and the larger 20-membered ring. The antimicrobial activities of the two polymers were tested by the agar diffusion method and the results indicated that they exhibited antimicrobial activities against bacterial strands. The measurement of the non-isothermal kinetics of the thermal decomposition of **2** reveals that there are at least three steps that occur in its decomposition process.

1. Introduction

The synthesis and investigation of new coordination polymers have been of great interest in the fields of crystal engineering and coordination chemistry recently owing to their intrinsic esthetic appeal and potential applications in various fields [1–6]. Over the last 10 years, researchers have reported numerous spectacular coordination polymers such as 1-D ladders and chains, 2-D grids, 3-D porous motifs, interpenetrated mode, and helical staircase networks [7–13], as well as explored their applications in catalysis, luminescent materials, NLO materials, phase transformation, host–guest chemistry, etc. [14–19]. However, in many cases it is quite difficult to synthesize desired metal-organic frameworks (MOFs) in a truly deliberate manner, since the kind of metal ions, the geometry of the organic ligands, the solvent and temperature [20–23] are all important factors to direct the self-assembly processes. Therefore, much more effort is required to extend our knowledge of the structural designing and to establish proper synthetic strategies that lead to the desired species with predictable structures and properties.

The selection of a suitable ligand is the key step in engendering MOFs with desirable dimension. It is generally accepted that rigid organic ligands may allow a controllable growth of the crystal structure [24,25]. In contrast, flexible organic ligands usually bring on structural diversification of the products, including the formation of supramolecular isomers [26,27]. Moreover, anions also play important roles in determining the structure of polymer, especially when the ligand is neutral. Some anions not only can act as counter anions to sustain neutral charge but also have various coordination modes to regulate frameworks. For example, the two-dimensional rhombohedral grid layered structure of $[Cd(btx)(SO_4)]$ (btx = 1,4-bis(triazol-1-ylmethyl)benzene) was ascribed to the abilities of btx and SO_4^{2-} to bridge between Cd centers [28]. However, some anions like PF_6^-, SbF_6^- or BF_4^- are often weakly coordinating anions and so metal–anion bonding interactions in their corresponding complexes were not thought to be structure determining. In summary, under appropriate reaction conditions, by choosing a suitable neutral organic ligand as the main ligand and a proper anion as well as a desirable metal ion, a complex with controlled structure could be designed.

Here, we selected a flexible *N*,*N*′-type ligand 1,1′-(1,3-propanediyl)bis-1H-benzimidazole (pbbm) and Cd(II) ion as framework-builders to assemble with framework-regulator SO_4^{2-} or ClO_4^- and obtained two new distinct coordination polymers, $[Cd(pbbm)_2(ClO_4)_2]_n$(**1**) with 1-D ribbon of rings and $\{[Cd(pbbm)SO_4(H_2O)_2]\cdot CH_3OH\}_n$(**2**) with 1-D looped chains composed of two kinds of rings. In addition, the non-isothermal kinetics of the thermal decomposition of polymer **2** was investigated. Since the biological activities of benzimidazole and its derivatives were reported in many literatures [29,30], we

* Corresponding author. Fax: +86 371 67761744.
E-mail address: houhongw@zzu.edu.cn (H. Hou).

0022-4596/$ - see front matter © 2008 Published by Elsevier Inc.
doi:10.1016/j.jssc.2008.04.045

determined the antimicrobial activities of the free ligand pbbm and polymers **1** and **2**.

2. Experimental section

2.1. General information and materials

All chemicals were of A.R. Grade and used without further purification. IR spectra were performed on a BRUKER TENSOR 27 spectrophotometer with KBr pellets in the 400–4000 cm^{-1} region. Carbon, hydrogen and nitrogen analyses were carried out on a FLASH EA 1112 elemental analyzer.

2.2. Preparation of the ligand 1,1′-(1,3-propanediyl)bis-1H-benzimidazole (pbbm)

Ligand 1,1′-(1,3-propanediyl)bis-1H-benzimidazole (pbbm) was prepared according to the literature [31]. Mp: 137–138 °C. Anal. Calcd for $C_{17}H_{16}N_4$(%): C, 73.89; H,5.84; N, 20.27. Found (%): C, 73.94; H, 5.92; N, 20.88. IR characteristics (KBr, cm^{-1}): 3095, 2396, 1500, 1457, 1390, 1287, 741, 635, 427.

2.3. Preparation of polymer $[Cd(pbbm)_2(ClO_4)_2]_n$(**1**)

A methanol solution of pbbm (5 ml, 55 mg, 0.2 mmol) was dropwise added into a methanol solution of $Cd(ClO_4)_2 \cdot 6H_2O$ (2 ml, 42 mg, 0.1 mmol). After filtration, the filtrate was allowed to stand in air at room temperature for about two weeks. Colorless single crystals suitable for X-ray diffraction were obtained in 50% yield. Anal. Calcd for $C_{34}H_{32}Cl_2CdN_8O_8$ (%): C, 47.26; H, 3.73; N, 12.97. Found (%): C, 47.48; H, 3.88; N, 13.13. IR characteristics (KBr, cm^{-1}): 3124, 2955, 1510, 1460, 1388, 1340, 1261, 1207, 1120, 1055, 750.

2.4. Preparation of polymer $\{[Cd(pbbm)SO_4(H_2O)_2] \cdot CH_3OH\}_n$(**2**)

A methanol solution of pbbm (5 ml, 55 mg, 0.2 mmol) was dropwise added into an aqueous solution of $3CdSO_4 \cdot 8H_2O$ (2 ml, 26 mg, 0.03 mmol) to give a clear solution. The resulting solution was allowed to stand in air at room temperature for about a week. Colorless single crystals suitable for X-ray diffraction were obtained in 55% yield. Anal. Calcd for $C_{18}H_{24}CdN_4O_7S$ (%): C, 39.10; H, 4.38; N, 10.13; S, 5.79. Found (%): C, 39.48; H, 4.29; N, 10.25; S, 5.87. IR characteristics (KBr, cm^{-1}): 3383, 3092, 2943, 1614, 1513, 1465, 1393, 1336, 1263, 1120, 1082, 1034, 980, 748, 617, 493, 431.

2.5. Crystal structure determination

The data were collected on a Bruker Aper CCD diffractomer with graphite monochromatic Mo$K\alpha$ radiation ($\lambda = 0.71073$ Å). A single crystal suitable for X-ray diffraction was mounted on a glass fiber. The data were collected at a temperature of 18 ± 1 °C and corrected for Lorenz-polarization effects. The structure was solved by direct methods and expanded using Fourier techniques. The non-hydrogen atoms were refined anisotropically and hydrogen atoms were included but not refined. The final cycle of full-matrix least-squares refinement is based on observed reflections and variable parameters. All calculations were performed using the SHELXL-97 crystallographic software package [32], and refined by full-matrix least-squares methods based on F^2. Table 1 shows crystallographic crystal data and structure processing parameters of complexes **1** and **2**. Selected bond lengths and bond angles of complexes **1** and **2** are listed in Table 2.

Table 1
Crystal data and structure refinement for polymers **1**–**2**

Polymers	**1**	**2**
Empirical formula	$C_{34}H_{32}CdCl_2N_8O_8$	$C_{18}H_{24}CdN_4O_7S$
Formula weight	863.98	552.87
Temperature (K)	291(2)	291(2)
Wavelength (Å)	0.71073	0.71073
Crystal system	Monoclinic	Triclinic
Space group	*P*2(1)/*c*	*P*-1
Unit cell dimensions		
a (Å)	8.7175(7)	9.0193(12)
b (Å)	19.2237(16)	11.0750(15)
c (Å)	10.4100(9)	12.8800(18)
α (deg)	90	66.646(2)
β (deg)	102.9450(10)	75.201(2)
γ (deg)	90	67.5560(10)
V (Å^3)	1700.2(2)	1083.4(3)
Z	2	2
D_{calc} (g/cm^3)	1.688	1.695
Absorption coefficient (mm^{-1})	0.866	1.152
F(000)	876	560
Crystal sizes (mm)	$0.37 \times 0.24 \times 0.16$	$0.24 \times 0.16 \times 0.08$
θ range (deg)	2.27–27.50	2.46–26.00
Index ranges	$-11 \leqslant h \leqslant 11$ $-24 \leqslant k \leqslant 24$ $-13 \leqslant l \leqslant 13$	$-11 \leqslant h \leqslant 11$ $-13 \leqslant k \leqslant 13$ $-15 \leqslant l \leqslant 11$
Reflns collected/unique [*R*(int)]	14854/3906 [0.0195]	6687/4001 [0.0234]
Data/restraints/params	3906/84/234	4001/6/298
GOF on F^2	1.025	1.019
Final *R* indices [$I > 2\sigma(I)$]	$R_1 = 0.0266$ $wR_2 = 0.0650$	$R_1 = 0.0308$ $wR_2 = 0.0595$
R indices (all data)	$R_1 = 0.0313$ $wR_2 = 0.0678$	$R_1 = 0.0387$ $wR_2 = 0.0637$
Largest diff peak and hole (e Å^{-3})	0.0562 and −0.374	0.370 and −0.474

Table 2
Selected bond lengths (Å) and angles (deg) for polymers **1**–**2**

Polymer **1**[a]			
Bond lengths			
Cd(1)–N(3)#1	2.2714(17)	Cd(1)–N(3)	2.2714(17)
Cd(1)–N(1)#1	2.4060(17)	Cd(1)–N(1)	2.4060(17)
Cd(1)–O(1′)#1	2.496(5)	Cd(1)–O(1)#1	2.517(5)
Bond angles			
N(3)#1–Cd(1)–N(3)	180.000(1)	N(3)–Cd(1)–N(1)#1	84.50(6)
N(3)#1–Cd(1)–N(1)	84.50(6)	N(3)–Cd(1)–N(1)	95.50(6)
N(1)#1–Cd(1)–N(1)	180.0	N(3)–Cd(1)–O(1′)#1	81.24(17)
N(1)–Cd(1)–O(1′)#1	84.22(18)	N(3)#1–Cd(1)–O(1′)	81.24(6)
N(3)–Cd(1)–O(1′)	98.76(6)	N(1)#1–Cd(1)–O(1′)	84.22(6)
N(1)–Cd(1)–O(1′)	95.78(6)	O(1′)#1–Cd(1)–O(1′)	180.0(2)
N(3)–Cd(1)–O(1)#1	93.46(17)	N(1)–Cd(1)–O(1)#1	98.01(19)
O(1′)–Cd(1)–O(1)#1	160.59(16)	N(3)#1–Cd(1)–O(1)	93.46(6)
N(3)–Cd(1)–O(1)	86.54(6)	N(1)#1–Cd(1)–O(1)	98.01(6)
N(1)–Cd(1)–O(1)	81.99(6)	O(1′)#1–Cd(1)–O(1)	160.59(16)
O(1′)–Cd(1)–O(1)	19.4	O(1)#1–Cd(1)–O(1)	180.0(2)
Polymer **2**[b]			
Bond lengths			
Cd(1)–N(4)#1	2.257(3)	Cd(1)–N(1)	2.258(2)
Cd(1)–O(1)	2.281(2)	Cd(1)–O(6)	2.363(2)
Cd(1)–O(5)	2.407(2)	Cd(1)–O(3)#2	2.411(2)
Bond angles			
N(4)#1–Cd(1)–N(1)	98.01(10)	N(4)#1–Cd(1)–O(1)	89.94(9)
N(1)–Cd(1)–O(1)	98.93(9)	N(4)#1–Cd(1)–O(6)	91.95(10)
N(1)–Cd(1)–O(6)	94.11(9)	O(1)–Cd(1)–O(6)	166.42(8)
N(4)#1–Cd(1)–O(5)	93.83(9)	N(1)–Cd(1)–O(5)	167.28(9)
O(1)–Cd(1)–O(5)	85.69(8)	O(6)–Cd(1)–O(5)	80.77(9)
N(4)#1–Cd(1)–O(3)#2	172.72(9)	N(1)–Cd(1)–O(3)#2	87.23(9)
O(1)–Cd(1)–O(3)#2	94.26(8)	O(6)–Cd(1)–O(3)#2	82.59(8)
O(5)–Cd(1)–O(3)#2	80.58(8)		

[a] Symmetry transformations used to generate equivalent atoms in polymer (**1**): #1 $-x+1, -y+1, -z+1$.

[b] Symmetry transformations used to generate equivalent atoms in polymer (**2**): #1 $-x, -y+1, -z+2$; #2 $-x-1, -y+2, -z+1$.

2.6. Thermal analysis

Thermal behaviors were measured on an NETZSCH TG209 instrument (Germany) in nitrogen atmosphere with a flow rate of 20 ml min^{-1}. The heating rate for thermal decomposition employed was 10 °C min^{-1}, and the rates for kinetic analysis were 10.0, 15.1, 20.3 and 25.5 °C min^{-1}, respectively. In kinetics experiments the precursor was pretreated in pure nitrogen atmosphere at 100 °C for 1 h to remove hydration water completely, and the range of temperature studied was from 250 to 650 °C.

2.7. Antimicrobial activity determination

As a preliminary screening for antimicrobial activity, we used the agar diffusion method as described in the literature [33]. Polymers **1** and **2** dissolved in DMF were tested against standard strains of *Staphylococcus aureus*, *Escherichia coli*, *Pseudomonas aeruginosa* and *Streptomyces griseus*, respectively. Nutrient agar (for *Streptomyces griseus*, there are glucose and peptone in nutrient agar) thawed by heating in a water bath was transferred to glass plates and frozen at about 37 °C. After test strains were spread on the solid nutrient agar surface, stainless steel tubes ($7.8 \times 6.0 \times 10\,mm^3$) were placed vertically on the surface. A total of 0.20 mL samples with a concentration of 5.0 g L^{-1} were injected to the steel tubes. They were allowed to incubate at 37 °C for 24 h (25 °C, 48 h for *Streptomyces griseus*). The inhibition zone around the disc was calculated as zone diameter in millimeters. Blank tests showed that DMF in the preparation of the test solutions does not affect the test organisms. All tests were repeated three times and average data were taken as the final result.

3. Results and discussion

3.1. Description of crystal structures

The structure of polymer **1** was evidenced by X-ray single-crystal diffraction. The coordination environment of the Cd(II) is shown in Fig. 1a. Each unit of **1** contains one Cd(II) center in which the Cd(II) ion coordinates to two oxygen atoms (O1A and O1) from two perchlorate anions and four nitrogen atoms (N1, N1A, N3 and N3A) from four pbbm ligands. Therefore, polymer **1** is neutral and the local coordination environment around Cd(II) can be described as a slightly distorted octahedron, in which four N atoms occupy the equatorial positions and two O atoms occupy the axial positions. The angles around the Cd(II) ion range are close to 90° or 180.0°, and the bond lengths around the Cd(II) ion range from 2.2714(17) Å to 2.517(5) Å (Table 2).

In polymer **1**, each $Cd(pbbm)_2(ClO_4)_2$ unit connects with two identical units through two bridging pbbm ligands, leading to the formation of the 1-D ribbon of rings. Two strands of pbbm ligands are wrapped around each other and held together by Cd(II) ions, forming double-stranded ribbons (Fig. 1b). The planar indexes of planes N3–N4–C11–C13 (1), C17–C16B–C15B (2), N1B–N2B–C3B–C5B (3) (Fig. 1a) are 0.0035, 0.0000 and 0.0293 Å, respectively. The dihedral angle between planes (1) and (2) is 70.5°, between planes (1) and (3) is 153.2° and between planes (2) and (3) is 109.8°. Herein, the pbbm ligand has twisted during coordinating. The ribbon of rings extended along the *a*-axis, and all of the Cd(II) ions in one chain are on the line strictly, the distance between two Cd(II) ions is 8.717 Å.

The crystal structure of **2** is significantly different from **1**; it displays an interesting infinite 1-D looped chains structure composed of two kinds of rings, the smaller 8-membered ring

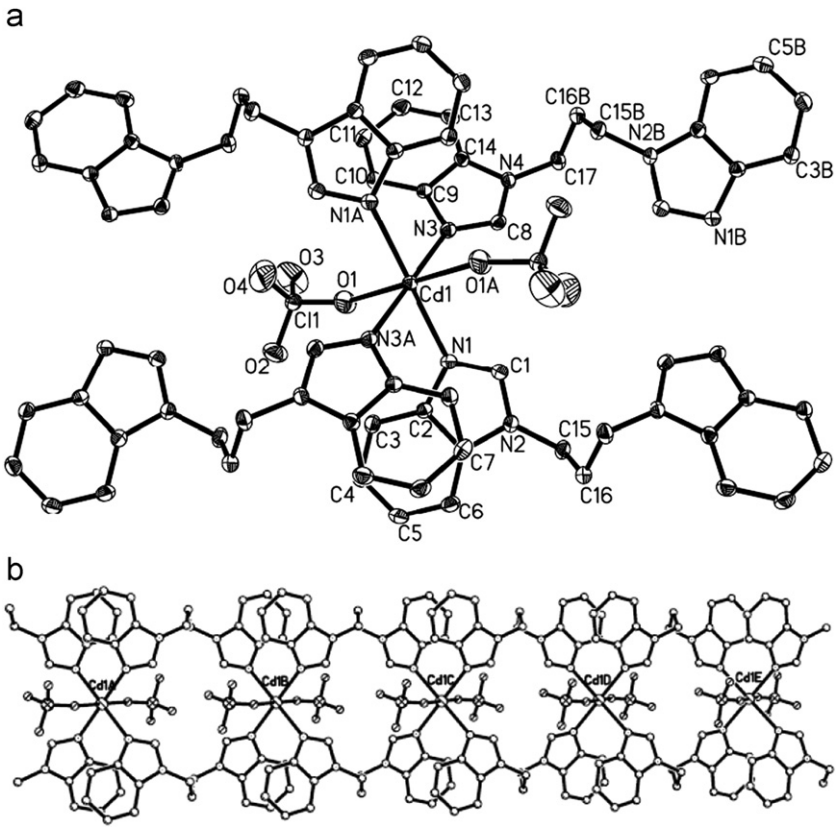

Fig. 1. (a) The coordination environment of the Cd(II) in polymer **1** with atom labeling scheme, showing 30% thermal ellipsoid. (b) The 1-D ribbon of the rings structure of polymer **1**.

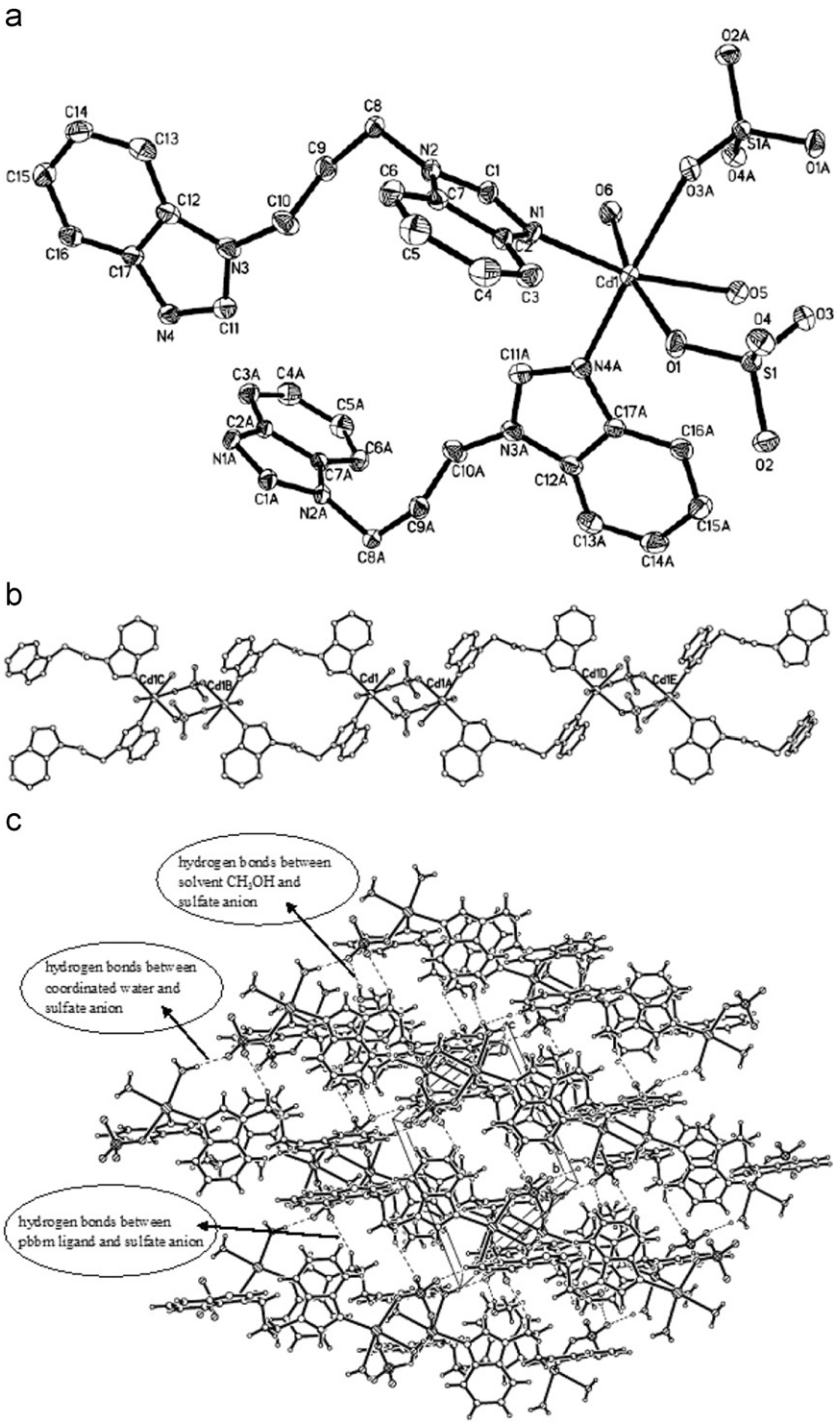

Fig. 2. (a) The coordination geometry of Cd(II) ion in polymer **2** with atom numberings, showing 30% thermal ellipsoid. (b) The 1-D looped chain structure of polymer **2**. (c) 3-D network of polymer **2** formed by hydrogen bonds.

and the larger 20-membered ring (Fig. 2b). The smaller ring is formed by two sulfate anions bridging two Cd(II) ions and the Cd(II)···Cd(II) distance is 4.988 Å. And the larger ring is made up of two pbbm molecules bridging two Cd(II) ions and the Cd(II)···Cd(II) distance is 10.629 Å. The above two kinds of rings are connected alternately via Cd(II) ions forming an infinite 1-D chain. These chains are parallel to each other and CH_3OH molecules are located in the interchain position. Moreover, the adjacent looped chains are linked through hydrogen bonds between coordinated waters and sulfate anions, solvent CH_3OH and sulfate anions, pbbm ligands and sulfate anions, resulting in a 3-D network (Fig. 2c).

The coordination geometry of the Cd(II) ion in **2** is shown in Fig. 2a. All of the pbbm ligands, sulfate anions and Cd(II) ions are equivalent, respectively. Each Cd(II) center is coordinated to two nitrogen atoms (N1, N4A) from two pbbm ligands, two oxygen atoms (O1, O3A) of sulfate anions and two oxygen atoms (O5, O6) from water molecules. The Cd1–O1 bond length is the shortest Cd–O bond and the Cd1–O3A bond length is the longest one. Atoms N1, O1, O5, O6 and Cd1 are nearly coplanar (the mean

deviation from plane is 0.0992 Å). The bond angle of N4A–Cd1–O3A is 172.72(9)°. Therefore, the local environment around Cd1 can be described as a distorted octahedral geometry.

3.2. Thermogravimetric analysis

The thermogravimetric analysis of polymer **2** was determined in the range of 25–700 °C in pure nitrogen atmosphere. The TG data from Fig. 3a show that the mass loss region from 60 to 120 °C is due to dehydration of the crystallized water molecules and free methanol molecules (obsd 11.66%, calcd 12.30%). Then a plateau region is observed from 120 to 360 °C. The successive mass loss from 360 to 660 °C may be attributed to the gradual elimination of loss of pbbm and sulfate anions. Finally a plateau region is observed from 660 to 700 °C. A brown residue of CdS remained (obsd 24.34%, calcd 26.11%).

The characterization frequencies of the IR spectra of polymer **2** as well as the decomposed products at 180 and 700 °C were determined with KBr pellets in the 400–4000 cm^{-1} region. The peak at 3383 cm^{-1} in the IR spectrum of polymer **2**, which is assigned to the characteristic OH stretching vibration, disappears in the spectrum of the decomposed product at 180 °C. The peaks at 3383, 1082, 1034 and 980 cm^{-1} in the IR spectrum of polymer **2**, which are attributed to the characteristic vibration bands of OH and SO_4^{2-}, disappear in the spectrum of the decomposed product at 700 °C. In order to examine the phase structure of the decomposed product of polymer **2** at 700 °C, the powders obtained after calcination were subjected to XRD analysis, and the results of which are shown in Fig. 3b (top). Fig. 3b shows that the powder calcined at 700 °C exhibits a diffraction pattern that matches the standard for hexagonal crystal CdS (Fig. 3b, bottom).

Kinetic parameter from TGA data may acquire additional insight into the mechanism of decomposition of polymer **2**. Hence, a series of dynamic scans with different heating rates results in a set of data. Based on these, two methods of differential and integral are developed by Friedman as well as Ozawa–Flynn–Wall to determine the kinetic parameters without having to presuppose a certain model. Fig. 4 shows the TG curves of polymer **2** measured in N_2 atmosphere with the heating rate of 10.0, 15.1, 20.3, 25.5 °C min^{-1}. The basic data (β,α,T) taken from the TG curves are used in the equations:

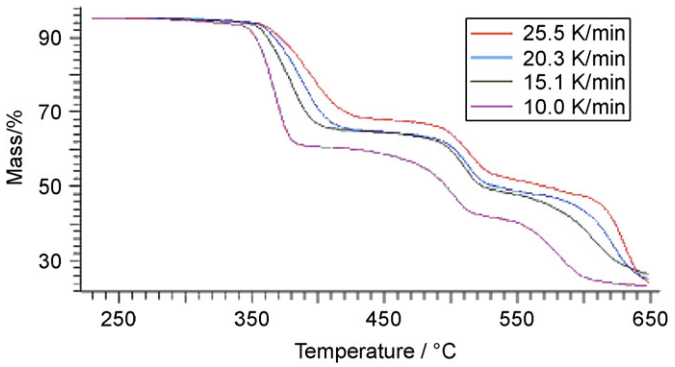

Fig. 4. The TG curves of polymer **2** measured in N_2 atmosphere with the heating rates of 10.0, 15.1, 20.3, 25.5 °C min^{-1}.

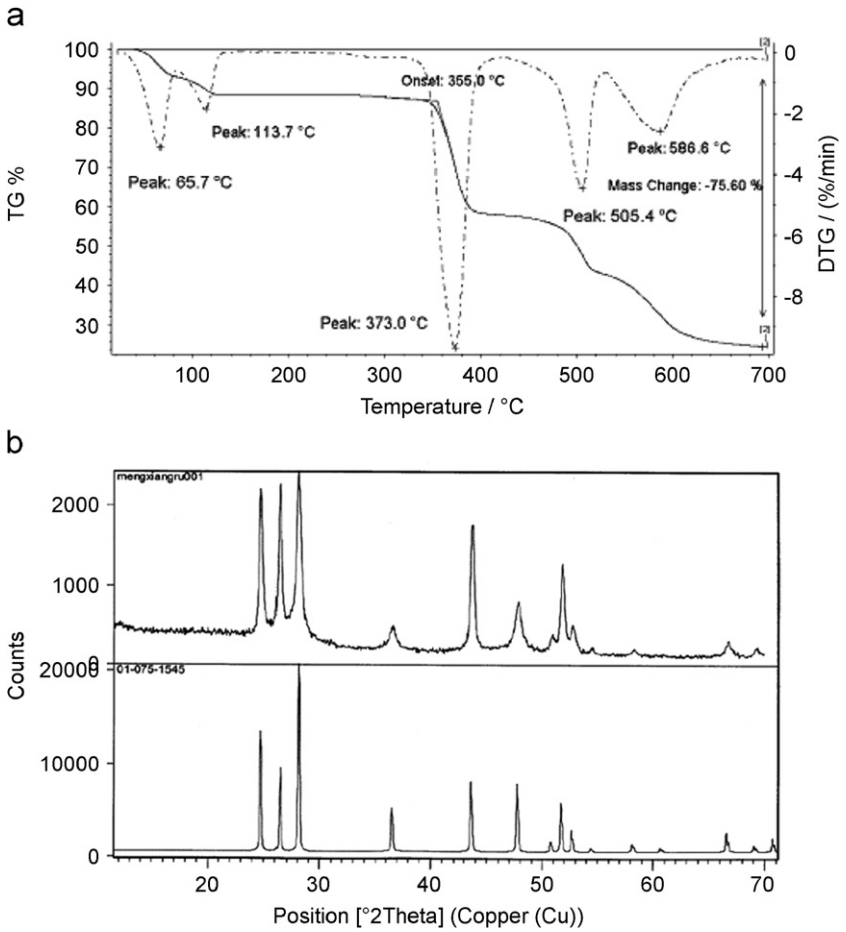

Fig. 3. (a) The TG-DTG curve of polymer **2** at 10 °C min^{-1} under nitrogen. (b) XRD patterns of the decomposed product of polymer **2** obtained at a temperature of 700 °C (top) and the standard XRD patterns for hexagonal crystal CdS (bottom).

- Ozawa–Flynn–Wall equation [34,35]

$$\ln \beta = \ln\left(\frac{AE}{R}\right) - \ln g(\alpha) - 5.3305 - 1.052\frac{E}{RT} \quad (1)$$

where β is the heating rate, α is the degree of conversion, $g(\alpha)$ is the mechanism function, E is the activation energy, A is the pre-exponential factor and R is the gas constant.

- Friedman equation [36]

$$\ln\left(\frac{d\alpha}{dt}\right)_{\alpha=\alpha_j} = \ln[Af(\alpha_j)] - \frac{E}{RT} \quad (2)$$

where $d\alpha/dt$ is the rate of conversion and $f(\alpha)$ is the mechanism function.

It can be seen from Eqs. (1) and (2) that the graphs $\ln\beta$ versus $1/T$ and $\ln(d\alpha/dt)$ versus $1/T$ both show straight lines with slopes $m_{(1)} = -1.052E/R$ and $m_{(2)} = -E/R$. The slopes of these straight lines are directly proportional to the reaction activation energy (E). Fig. 5 shows these lines at different α by means of the OFW method, and Fig. 6 shows Friedman analysis of the decomposition process of polymer **2**. The calculated results using both Eqs. (1) and (2) are shown in Table 3.

As shown in Table 3 the values of activation energy obtained by the two methods are in reasonable agreement with each other and it changes with the degree of conversion. We know that the variation of activation energy demonstrated the complexity of the decomposition process. As can be seen from Table 3, the activation energy values increase from 82.90 to 173.67 kJ mol^{-1} in the 0.02–0.05 range extent of conversion, decrease from 173.67 to 24.20 kJ mol^{-1} in the 0.05–0.40 range, increase from 24.20 to 90.93 kJ mol^{-1} in the 0.40–0.60 range, decrease from 90.93 to 41.26 kJ mol^{-1} in the 0.60–0.70 range and increase from 41.26 to 144.26 kJ mol^{-1} in the 0.70–0.98 range (OFW method). By all appearance, three maximums appear with the test extent of decomposition. This behavior allows us to hypothesise that at least three steps occur in the decomposition process. According to the OFW method, the activation energy and pre-exponential factors of thermal decomposition of polymer **2** are, $E_1 = 173.67 \pm 9.45$ kJ mol^{-1}, $\lg(A_1/s^{-1}) = 11.25$, $E_2 = 90.93 \pm 13.43$ kJ mol^{-1}, $\lg(A_2/s^{-1}) = 3.74$, and $E_3 = 144.26 \pm 40.28$ kJ mol^{-1}, $\lg(A_3/s^{-1}) = 6.73$, respectively.

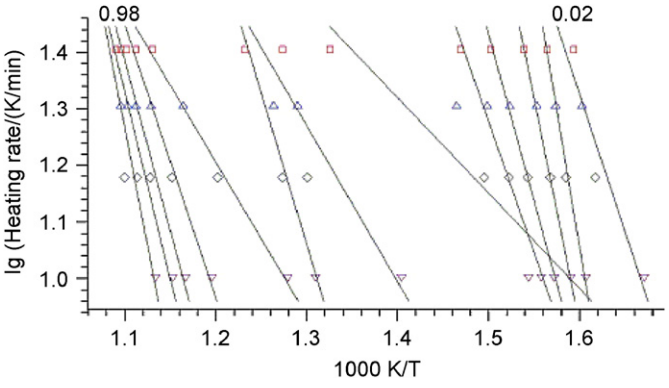

Fig. 5. Ozawa–Flynn–Wall analysis of the decomposition process of polymer **2**.

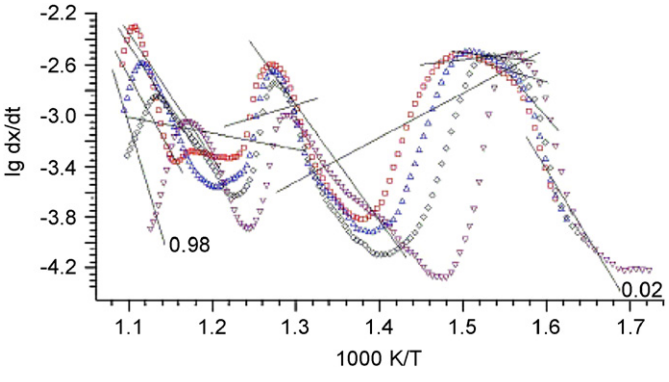

Fig. 6. Friedman analysis of the decomposition process of polymer **2**.

Table 3
Parameters E (kJ mol^{-1}) and lg(A/s^{-1}) for the thermal decomposition of polymer **2**

Partial mass loss	Ozawa–Flynn–Wall analysis		Friedman analysis	
	E/(kJ mol^{-1})	lg (A/s^{-1})	E/(kJ mol^{-1})	lg (A/s^{-1})
0.02	82.90 ± 16.47	3.24	206.94 ± 28.18	13.88
0.05	173.67 ± 9.45	11.25	144.11 ± 23.60	9.06
0.10	141.29 ± 2.94	8.64	39.57 ± 7.65	0.61
0.20	102.38 ± 3.95	5.51	13.71 ± 4.06	−1.34
0.30	78.82 ± 4.98	3.61	−16.26 ± 12.86	−3.68
0.40	24.20 ± 8.17	−1.07	−66.92 ± 7.66	−7.85
0.50	42.97 ± 12.09	0.29	174.84 ± 16.97	9.26
0.60	90.93 ± 13.43	3.74	−37.75 ± 120.41	−5.08
0.70	41.26 ± 2.47	0.06	23.96 ± 54.13	−1.11
0.80	79.56 ± 5.61	2.58	188.04 ± 40.29	9.15
0.90	102.07 ± 13.50	4.06	196.06 ± 58.41	9.82
0.98	144.26 ± 40.28	6.73	424.83 ± 125.67	23.05

Table 4
Diameter of inhibition zone (mm)

Compound	*Staphylococcus aureus*	*Escherichia coli*	*Pseudomonas aeruginosa*	*Streptomyces griseus*
Ligand pbbm	16	14	14	15
Polymer **1**	24	18	18	20
Polymer **2**	23	18	18	24
Blank	8	10	9	10

At high temperature, polymer **1** can lead to uncontrollable reactions with consequent danger situations, so we do not measure its thermal behaviors.

3.3. Antimicrobial activity

In our previous work, we have determined the number average molecular weights (M_n) and weight average molecular weights (M_w) of this kind of polymers in DMF solution and found that they are not dissociated in DMF solution. Thus, we confirm that the skeleton of polymers **1** and **2** is intact in DMF solution [37–39]. So the antimicrobial activities in the DMF solutions of polymers **1** and **2** can represent the antimicrobial activities of polymers **1** and **2**. The results of antimicrobial activities of the two complexes and the free ligand pbbm, together with the result of the blank as a comparison, are listed in Table 4, as evaluated by the diameter of the inhibition zone around each disc. It can be seen from Table 4 that the free ligand pbbm shows slender antimicrobial activity. After complexation with Cd(II), the antimicrobial activity of the complexes (both **1** and **2**) are stronger than that of the free ligand. This fact may indicate that the metal center is an essential factor to increase the antibacterial activities. Through comparing activities of polymers **1** and **2**, we found that they possess similar activities against *Staphylococcus aureus*, *Escherichia coli* and *Pseudomonas aeruginosa*, but polymer **2** shows higher activity against *Streptomyces griseus* than that of **1**. The mechanism of

antimicrobial activities of these compounds still needs further study and the experimental results above would provide basic data for the pharmacological research of bis-benzimidazole-type ligands and their complexes.

4. Conclusions

In short, we have prepared and characterized two new 1-D chain frameworks with different structures based on the same framework-builders 1,1′-(1,3-propanediyl)bis-1H-benzimidazole, Cd(II) ion and different framework-regulator ClO_4^- or SO_4^{2-}. This indicates that we can manipulate polymeric structures through modulation of the counter anions. The data from the antimicrobial activity determination reveal that the antimicrobial activities of these complexes are stronger than that of the free ligand pbbm. It implies that the central metal ion may be an essential factor to increase the antibacterial activities.

Acknowledgments

The authors acknowledge financial support from the National Natural Science Foundation of China (Nos. 20671082) and NCET.

Appendix A. Supplementary data

Crystallographic data in CIF format have been deposited at the Cambridge Crystallographic Data Centre with CCDC numbers 678893 and 678894. Copies of this information may be obtained free of charge from the Director, CCDC, 12 Union Road, Cambridge CB2 1EZ, UK (fax: +44 1223 336033; e-mail: deposit@ccdc.cam.ac.uk; or http://www.ccdc.cam.ac.uk).

Appendix B. Supplementary Materials

Supplementary data associated with this article can be found in the online version at doi:10.1016/j.jssc.2008.04.045.

References

[1] H.W. Hou, Y.L. Wei, Y.L. Song, L.W. Mi, M.S. Tang, L.K. Li, Y.T. Fan, Angew. Chem. Int. Ed. Engl. 117 (2005) 6221.
[2] G.Q. Zhang, G.Q. Yang, J.S. Ma, Cryst. Growth Des. 6 (2006) 1897.
[3] J.J. Perry, G.J. McManus, M.J. Zaworotko, Chem. Commun. (2004) 2534.
[4] Z.B. Han, X.N. Cheng, X.M. Chen, Cryst. Growth Des. 5 (2005) 695.
[5] V.V. Smirnov, J.P. Roth, J. Am. Chem. Soc. 128 (2006) 3683.
[6] R. Matsuda, R. Kitaura, S. Kitagawa, Y. Kubota, R.V. Belosludov, T.C. Kobayashi, H. Sakamoto, T. Chiba, M. Takata, Y. Kawazoe, Y. Mita, Nature 436 (2005) 238.
[7] K. Nomiya, H Yokoyama, J. Chem. Soc. Dalton Trans. (2002) 2483.
[8] D.M. Shin, I.S. Lee, Y.A. Lee, Y.K. Chung, Inorg. Chem. 42 (2003) 2977.
[9] G.X. Ma, T.L. Zhang, J.G. Zhang, K.B. Yu, Z. Anorg. Allg. Chem. 630 (2004) 423.
[10] R. Wang, E. Gao, M. Hong, S. Gao, J. Luo, Z. Lin, Inorg. Chem. 42 (2003) 5486.
[11] C.D. Wu, C.Z. Lu, H.H. Zhuang, J.S. Huang, J. Am. Chem. Soc. 124 (2002) 3836.
[12] M. Eddaoudi, J. Kim, N. Rosi, D. Vodak, J. Wachter, M. O'Keeffe, O.M. Yaghi, Science 295 (2002) 469.
[13] T.M. Reineke, M. Eddaoudi, D. Moler, M. O'Keeffe, O.M. Yaghi, J. Am. Chem. Soc. 122 (2000) 4843.
[14] O.M. Yaghi, G. Li, H. Li, Nature 378 (1995) 703.
[15] M. Eddaoudi, H. Li, O.M. Yaghi, J. Am. Chem. Soc. 122 (2000) 1391.
[16] T.M. Madkour, R.A. Azzam, J.E. Mark, J. Polym. Sci. B: Pol. Phys. 44 (2006) 2524.
[17] G.D. Paoli, Z. Džolic, F. Rizzo, L.D. Cola, F. Vögtle, W.M. Müller, G. Richardt, M. Žinic, Adv. Funct. Mater. 17 (2007) 821.
[18] A.R. Timerbaev, L.S. Foteeva, A.V. Rudnev, J.K. Abramski, K. Poteć-Pawlak, C.G. Hartinger, M. Jarosz, B.K. Keppler, Electrophoresis 28 (2007) 2235.
[19] R.W. Saalfrank, R. Burak, S. Reihs, N. Low, F. Hampel, H.D. Stachel, J. Lentmaier, K. Peters, E.M. Peters, H.G. von Schnering, Angew. Chem. Int. Ed. Engl. 34 (1995) 993.
[20] M.B. Zaman, M.D. Smith, H.C. zur Loye, Chem. Commun. (2001) 2256.
[21] D.L. Reger, T.D. Wright, R.F. Semeniuc, T.C. Grattan, M.D. Smith, Inorg. Chem. 40 (2001) 6212.
[22] H.B. Chen, H. Zhang, J.M. Yang, Z.H. Zhou, Polyhedron 23 (2004) 987.
[23] M.A. Withersby, A.J. Blake, N.R. Champness, P.A. Cooke, P. Hubberstey, W.S. Li, M. Schröder, Inorg. Chem. 38 (1999) 2259.
[24] L.P. Wang, X.R. Meng, E.P. Zhang, H.W. Hou, Y.T. Fan, J. Organomet. Chem. 692 (2007) 4367.
[25] J.H.N. Buttery, Effendy, G.A. Koutsantonis, S. Mutrofin, N.C. Plackett, B.W. Skelton, C.R. Whitaker, A.H. White, Z. Anorg. Allg. Chem. 632 (2006) 1829.
[26] B.L. Wu, M.Y. Wu, Y.Q. Gong, B.Q. Chen, M.C. Hong, Jiegou Huaxu (Chin. J. Struct. Chem.) 25 (2006) 511.
[27] B.L. Wu, D.Q. Yuan, B.Y. Lou, L. Han, C.P. Liu, C.X. Zhang, M.C. Hong, Inorg. Chem. 44 (2005) 9175.
[28] X.R. Meng, Y.L. Song, H.W. Hou, H.Y. Han, B. Xiao, Y.T. Fan, Y. Zhu, Inorg. Chem. 43 (2004) 3528.
[29] F. Saczewski, E. Dziemidowicz-Borys, J.B. Patrick, R. Grünert, M. Gdaniec, P. Tabin, J. Inorg. Biochem. 100 (2006) 1389.
[30] A.A. Spasov, I.N. Yozhitsa, L.I. Bugaeva, V.A. Anisimova, Pharm. Chem. J. 33 (1999) 232.
[31] X.J. Xie, G.S. Yang, L. Cheng, F. Wang, Huaxue Shiji (Chin. Ed.) 22 (2000) 222.
[32] G.M. Sheldrick, SHELXL-97, Program for Refinement of Crystal Structure, University of Göttingen, Germany, 1997.
[33] K.S. Lu, Y.C. Xu, H. Yu, Y. Shi, Zhongguo Huanjing Jiance (Environmental Monitoring in China) 7 (1991) 9.
[34] T. Ozawa, Bull. Chem. Soc. Japan 38 (1965) 1881.
[35] J.H. Flynn, L.H. Wall, Polym. Lett. 4 (1966) 323.
[36] H.L. Friedman, J. Res. Nat. Bur. Stds. 57 (1965) 217.
[37] H.W. Hou, X.R. Meng, Y.L. Song, Y.T. Fan, Y. Zhu, H.J. Lu, C.X. Du, W.H. Shao, Inorg. Chem. 41 (2002) 4068.
[38] H.W. Hou, Y.L. Wei, Y.L. Song, Y. Zhu, L.K. Li, Y.T. Fan, J. Mater. Chem. 12 (2002) 838.
[39] X.M. Meng, Y.L. Song, H.W. Hou, Y.T. Fan, G. Li, Y. Zhu, Inorg. Chem. 42 (2003) 1306.